Table 3. *Interatomic distances* (Å) *in* Bi *polyhedra of* $Bi_{12}GeO_{20}$ *and* γ-Bi_2O_3

	$Bi_{12}GeO_{20}$	γ-Bi_2O_3
Bi—O(1^{i})	2.072 (1)	2.045 (3)
Bi—O(1^{ii})	2.221 (1)	2.402 (3)
Bi—O(1^{iii})	2.622 (1)	2.456 (3)
Bi—O(2)	2.2146 (6)	2.278 (3)
Bi—O(3^{iv})	2.6241 (8)	2.561 (3)

Symmetry codes: (i) $\frac{1}{2}-x, \frac{1}{2}-y, -\frac{1}{2}+z$; (ii) y, z, x; (iii) $y, 1-z, -x$; (iv) $1-x, 1-y, -1+z$.

bond lengths are shorter by 0.17 and 0.06 Å, while the Bi—O(1^{ii}) and Bi—O(2) bond lengths are longer by 0.18 and 0.06 Å, respectively, as compared to similar bond lengths in $Bi_{12}GeO_{20}$.

A detailed comparison of the geometries of Bi polyhedra in the structures of $Bi_{12}GeO_{20}$ (Radaev, Muradyan, Simonov, Sarin *et al.*, 1990) and (Bi,Fe), (Bi,Zn) sillenites (Radaev, Muradyan & Simonov, 1990) which also exhibit O(3)-atom deficiency revealed changes in the Bi—O bond lengths in the latter, similar to the changes considered in this work: the Bi—O(3) bonds were shortened while the Bi—O(1^{ii}) bonds were lengthened as compared to similar ones in $Bi_{12}GeO_{20}$. This fact is indirect evidence of the above-suggested atomic model of γ-phase Bi_2O_3.

The authors are most grateful to Dr V. P. Glazkov and Professor V. A. Somenkov for their assistance with data collection and Dr Arzamastsev for useful advice. The authors would also like to thank Professor R. A. Young for supplying the programs for full-profile analysis.

Out studies of sillenites were stimulated by the work of Dr L. A. Muradyan. The γ-phase Bi_2O_3 model reported in Radaev, Muradyan & Simonov (1990) was suggested by her. We most profoundly regret her sudden death in December 1989. We would like to dedicate this work to her memory.

References

ABRAHAMS, S. C., BERNSTEIN, J. L. & SVENSSON, C. (1979). *J. Chem. Phys.* **71**, 788–792.

AURIVILLIUS, B. & SILLEN, L. G. (1945). *Nature (London)*, **155**, 305–306.

CRAIG, D. C. & STEPHENSON, N. S. (1975). *J. Solid State Chem.* **15**, 1–8.

GLAZKOV, V. P., NAUMOV, I. V., SOMENKOV, V. A. & SHILSTEIN, S. SH. (1988). *Nucl. Instrum. Methods Phys. Res.* A**264**, 367–374.

HARWIG, H. A. (1978). *Z. Anorg. Allg. Chem.* **444**, 151–166.

MURADYAN, L. A., RADAEV, S. F. & SIMONOV, V. I. (1989). *Methods of Structural Analysis*, pp. 5–20. Moscow: Nauka.

RADAEV, S. F., MURADYAN, L. A., KARGIN, YU. F., SARIN, V. A., RIDER, E. E. & SIMONOV, V. I. (1989*a*). *Dokl. Akad. Nauk SSSR*, **306**, 624–627.

RADAEV, S. F., MURADYAN, L. A., KARGIN, YU. F., SARIN, V. A., RIDER, E. E. & SIMONOV, V. I. (1989*b*). *Dokl. Akad. Nauk SSSR*, **307**, 1381–1384.

RADAEV, S. F., MURADYAN, L. A., SARIN, V. A., KANEPIT, V. N., YUDIN, A. N., MAR'IN, A. A. & SIMONOV, V. I. (1989). *Dokl. Akad. Nauk SSSR*, **307**, 606–610.

RADAEV, S. F., MURADYAN, L. A & SIMONOV, V. I. (1990). *Acta Cryst.* B**47**, 1–6.

RADAEV, S. F., MURADYAN, L. A., SIMONOV, V. I., SARIN, V. A., RIDER, E. E., KARGIN, YU. F., VOLKOV, V. V. & SKORIKOV, V. M. (1990). *Vysokochistye Veshestva*, **2**, 158–164.

RIETVELD, H. M. (1969). *J. Appl. Cryst.* **2**, 65–71.

SCHUMB, W. C. & RITTNER, E. S. (1943). *J. Am. Chem. Soc.* **65**, 1055–1060.

SILLEN, L. G. (1937). *Ark. Kemi. Mineral. Geol.* A**128**, 1–15.

SVENSSON, C., ABRAHAMS, S. C. & BERNSTEIN, J. L. (1979). *Acta Cryst.* B**35**, 2687–2690.

WATANABE, A., KODAMA, H. & TAKENOUCHI, S. (1990). *J. Solid State Chem.* **85**, 76–82.

WILES, D. B. & YOUNG, R. A. (1981). *J. Appl. Cryst.* **14**, 149–151.

Acta Cryst. (1992). B**48**, 609–622

Applications and Limitations of the Ionic Potential Model with Empirically Derived Ion-Specific Repulsion Parameters

BY MARTIN KUNZ AND THOMAS ARMBRUSTER

Laboratorium für chemische und mineralogische Kristallographie, Universität Bern, Freiestr. 3, CH-3012 Bern, Switzerland

(*Received* 4 *October* 1991; *accepted* 30 *March* 1992)

Abstract

A consistent set of ion-specific short-range repulsion parameters (A and B) has been assessed using the potential-energy minimization program *WMIN*. The values of the 'softness parameters' B were determined by quadratic extrapolation from isoelectronic species previously derived from vibrational data. The repulsion radii, A, were refined from known crystal structures minimizing their lattice energy while B was kept invariant. Repulsion radii and softness parameters show reasonable corre-

0108-7681/92/050609-14$06.00

lations with chemical and physical properties through the periodic table of elements. The new set of short-range repulsion parameters was used to model ionic crystal structures with satisfactory accuracy when compared with coordinates and resulting interatomic distances of structures refined from diffraction experiments. As test structures, Mg_2SiO_4 and $MgSiO_3$ polymorphs were compared with previous ionic potential models. Corundum-type structures were successfully applied to model the ionic repulsion across face-sharing octahedra. Less successfully, Ti-containing compounds were used to test the ability of the ionic model to predict polyhedral distortions around Ti^{4+} cations. A complementary approach, based on the bond-valence model, is applied to explain polyhedral distortions of Ti^{4+} coordinations where a simple ionic approach fails.

Introduction

During the past few years, the ionic potential model has been successfully used for the simulation of crystal structures including their chemical and physical properties. The ionic model describes the lattice energy of a crystal as the sum of Coulomb and dispersion interactions (van der Waals forces) plus a short-range repulsive term. A crystal structure is supposed to be stable when this sum reaches a minimum. The calculation of the Coulomb energy can be done straightforwardly by summation over all possible interactions within the crystal with the methods of Ewald (1921) or Bertaut (1952).

The effective dispersion or van der Waals interaction involves a r^{-6} term and a constant which can be estimated according to Margenau (1939) with the ionization energy and the electronic polarizability of the respective ions. The evaluation of the electronic polarizability is often difficult since only very limited data are available (*e.g.*, Lasaga & Cygan, 1982). However, the van der Waals term can be neglected in many cases as it is very small compared to the Coulomb term.

The short-range repulsive term on the other hand cannot be neglected owing to its balancing effect on the equilibrium structure. Thus, one of the main problems for the application of the ionic model to simulate crystal structures and properties is to find a suitable way of describing the short-range repulsion force (Burnham, 1990). Since the short-range interactions are not as straightforward to handle as the Coulomb interactions, various approaches exist to quantify the repulsive contribution of the lattice energy.

The Born–Mayer parameterization (Born & Mayer, 1932) describes the repulsive energy with an exponential form related to the exponential decrease of the electron density probability with increasing distance:

$$W_{ij}(\text{rep}) = \lambda_{ij}\exp(-r_{ij}/\rho_{ij}),$$

where λ_{ij} and ρ_{ij} are ion-pair-specific constants for the ions i and j, and r_{ij} represents the internuclear distance between atoms i and j. The constants of the Born–Mayer form have to be evaluated for each atom pair occurring in the structure to be simulated.

An extension of the Born–Mayer approach is the so-called Buckingham parameterization. It adds to the exponential term an attractive van der Waals term proportional to r^{-6} with again an ion-pair-specific constant C_{ij}.

A variation of the pair-potential approach of Born & Mayer (1932) is the ion-specific modification given by Gilbert (1968):

$$W_{ij}(\text{rep}) = f_0(B_i + B_j)\exp[(A_i + A_j - r_{ij})/(B_i + B_j)].$$

Here, the parameters A and B are constants specific to each ion and r_{ij} stands for the internuclear distance between ions i and j. The constant f_0 represents a standard force (Gilbert, 1968; Busing, 1970) with a numerical value of 1 and units of kcal mol^{-1} $Å^{-1}$. Therefore, the Gilbert parameters A_i and B_i have the dimension of a length with units of Å. It should be mentioned that the Gilbert-type parameters A_i and B_i are in principle equivalent to the pair-specific parameters of Born & Mayer (1932) and can be transformed *via* the following relations:

$$(A_i + A_j) = \rho_{ij}\ln(\lambda_{ij}/\rho_{ij})$$

$$(B_i + B_j) = \rho_{ij}.$$

The advantage of the ion-specific form of Gilbert (1968) is the fact that, after having determined A and B for all ions of interest, each possible interaction between these atoms can be modeled without evaluating two constants for each pair interaction individually, which reduces the amount of parameters to be determined from $2\binom{n}{2}$ to $2n$ (n = number of ion species).

Common to all these parameterizations is the necessity to supply values for the constants introduced. In principle, there are two different ways to evaluate these constants.

(1) The values may be determined empirically by fitting the variables to observable quantities such as vibrational spectra, bulk compressibility or structural arrangements.

(2) The variables may be derived by theoretical models: Gordon & Kim (1972) developed a method which describes forces between closed-shell atoms in terms of the electron-gas theory. Their initial theory was modified by Waldmann & Gordon (1979) and Mulhausen & Gordon (1981) to the modified electron gas (MEG) theory. Lasaga & Gibbs (1987,

1988) determined pair potentials *ab initio* with quantum mechanical molecular orbital calculations. In these cases, the potential parameters are determined by fitting them to the interatomic potentials calculated with MEG or quantum mechanics, respectively.

In spite of the remarkable success of the MEG approach, empirically fitted constants may be more suitable for certain problems. The MEG theory, being a purely ionic approach, is not able to take special bonding properties into account such as anisotropic polarizability or covalence effects. Covalent bonds were considered by Lasaga & Gibbs (1987, 1988, 1991) for hydroxyacid polymers of silicate tetrahedra. However, this method will require enormous computational efforts for more complicated structural units.

Empirically determined constants on the other hand have all bonding properties incorporated by the very nature of their determination. However, simultaneous fitting of two or more parameters to an observed structure may be affected by correlation problems, especially if the region of the energy minimum represents a flat potential surface. Thus, fitting repulsion parameters of the same atom or the same atom pair to different structures may well lead to different parameter pairs. It is clear from this point of view that such repulsion parameters can hardly correlate with any systematic physical or chemical trends of the respective ions within the periodic table, though such correlations have to be expected for physically reasonable parameters. Also, these parameters show only poor transferability between different structure types. For instance, parameters of Mg, Si and O fitted to the α-Mg_2SiO_4 structure work well for the 'source' structure, but modeling of ilmenite-type $MgSiO_3$ using these parameters yields less satisfactory agreement with the observed structural arrangement (Miyamoto & Takeda, 1984).

Hence, a consistent set of empirically fitted constants which could be applied to a variety of structure types might well be desirable in order to simulate crystal structures of various chemical compositions. It is the goal of this work to establish a set of Gilbert-type ion-specific repulsion parameters which enable structural modeling of various structure types with various chemical compositions. In addition, such consistent repulsion parameters are expected to correlate with ionic properties within the periodic table of elements. Applications of these parameters to various structure types will demonstrate their transferability and limitations.

Previous work

An enormous amount of work has been published on the general topic of crystal structure modeling with the ionic model. Excellent overviews, for example, are given by Burnham (1985, 1990) and Catlow & Price (1990). However, little work has been done on Gilbert-type repulsion parameters: Busing (1970) uses the Gilbert parameterization to fit repulsion parameters and crystal structures of alkaline-earth chorides with the program *WMIN* (Busing, 1981). The same program was used by Miyamoto & Takeda (1980, 1984), Matsui & Busing (1984) and Price & Parker (1984) to refine repulsion parameters of Mg, Si and O, which were subsequently used to model mantle minerals. However, comparing the values of the same variables determined by different authors, one finds conspicuous differences. Nevertheless, all parameter pairs are able to simulate Mg-silicate structures to a similar accuracy. In addition, comparison of ion-specific repulsion parameters calculated from MEG-derived pair-specific constants (Post & Burnham, 1986) with the above-cited values reveals significant deviations. These differences between repulsion-parameter pairs for equivalent atoms in identical structure types support the presumption that these least-squares refinements are affected by strong correlations and thus do not lead to a global minimum if the potential surface is flat in the minimum region.

Lasaga & Gibbs (1987, 1988) applied *ab initio* calculated ionic potentials to silicate hydroxyacid polymers. Their calculations showed that a purely ionic model is not able to predict all the special features of Si—O bonds. These effects were modeled with three-body angle-bending terms. An approach with reduced charges did not lead to an improvement in the results. Lasaga & Gibbs (1987) show that covalent effects may be neglected for orthosilicates, where the metal–oxygen interaction seems to dominate the structural pattern.

Procedure for repulsion-parameter determination

Using the program *WMIN* (Busing, 1981), we have developed a consistent set of Gilbert-type repulsion parameters for a variety of closed-shell and first-row transition elements. *WMIN* is programmed to calculate and minimize lattice energies for the determination of various parameters (repulsion, van der Waals) as well as equilibrium structures. We used the program in its original version applying the Ewald (1921) method to accelerate convergence of the Coulomb summation. The repulsion term is parameterized after Gilbert (1968) using ion-specific repulsion parameters A and B, where A can be visualized as a repulsion radius and B represents a measure of the softness of the ion. Since the evaluation of van der Waals terms is affected by some uncertainties (*e.g.* Busing, 1970), we decided to omit van der Waals terms in the energy calculation to avoid additional error sources. It has generally to be kept in

mind that the aim of this work is primarily to establish a consistent set of short-range repulsion parameters. Thus, we applied a pure two-body soft-sphere model in order to exclude additional error sources which might be inherent in the inclusion of polarization and/or three-body terms. The neglection of a polarization term [*e.g.* shell model after Dick & Overhauser (1958)] may be justified by the only small perturbation which ionic polarizability causes in structures (Parker, 1982). An inclusion of three-body terms is desirable *e.g.* for the simulation of tetrahedral framework structures and SiO_2 polymorphs (*e.g.* Lasaga & Gibbs, 1987, 1988). However, since these terms apply primarily to angle effects of highly directed covalent bonds, they will not have much influence on the value of the repulsion parameters. In addition, three-body terms may reasonably be neglected for the treatment of orthosilicates, where the Si—O bond shows up to 75% ionicity (Parker, 1982, and references therein).

To circumvent the above-described correlation problems, we refined only one parameter for each structure. This implies an independent assessment of one of the two repulsion parameters A and B for all elements as well as an initial determination of both parameters for one backbone element. Having done this, the remaining repulsion parameters of various elements can be fitted to the structures of binary compounds containing the backbone atom. In a more advanced stage, ternary or quaternary compounds with elements previously determined were also used.

We decided to fix the B parameters of all elements by physical reasoning and to refine only the A parameters with *WMIN* where cell parameters and coordinates were used as observations. As an exception, A and B of oxygen as our backbone element were obtained from the pair-specific constants given for the O–O interaction by Lasaga & Gibbs (1987).

A similar approach was adopted by Lewis & Catlow (1985) to determine pair-specific constants (λ and ρ) for oxides where little experimental data were available, *i.e.* transition-element oxides. The latter authors were able to demonstrate that the approximation of fixing one repulsion parameter yields encouraging results and is comparable to more sophisticated methods.

Determination of the *B* parameter

To evaluate a reasonable set of softness parameters B, the following highly simplifying assumptions were made:

(1) The softness of an ion is an expression of the repulsive interaction of the valence electrons within the valence shell and therefore indirectly proportional to the valence-electron density of the ion.

(2) Valence electrons of a closed-shell ion are considered to be distributed on a spherical surface which has a quadratic relationship to the radius of the valence shell ($4\pi r^2$).

(3) The radius of the valence shell decreases linearly with atom number Z for ions with the same electron configuration (isoelectronic ions) due to stronger nucleus–electron attraction. It will be shown below that this relationship of the valence-shell radii is reflected in the repulsion radii.

Thus, the valence-electron density and therefore the hardness of the ion increases quadratically with increasing Z within an isoelectronic series. Conversely, the softness parameters B of an isoelectronic row are therefore expected to decrease along a quadratic curve.

B values calculated from spectroscopic data by Gilbert (1968) for alkali, noble-gas and halide ions as well as extrapolated values for alkaline-earth ions (Busing, 1970) and the *ab initio* value of oxygen (Lasaga & Gibbs, 1987) were used to fit quadratic regression curves to the following isoelectronic rows:

Ne row: including all ions with Ne electron configuration (O^{2-} to S^{6+}).

Ar row: ions with Ar electron configuration (Cl^- to Se^{6+}, without first-row transition metals).

Kr row: main-group ions with Kr electron configuration [Br^- to Te^{6+}; no data for B(Kr) given, $B(Br^-)$ extrapolated from $B(F^-)$ and $B(Cl^-)$].

Xe row: main-group ions with Xe electron configuration [I^- to Bi^{5+}; no data for B(Xe) given; $B(I^-)$ extrapolated from $B(F^-)$ and $B(Cl^-)$].

For these quadratic regression analyses of the values given by Gilbert (1968) and Busing (1970), the B value of the next-heaviest noble gas was constrained to be 0. Thus, for example, a hypothetical Ar^{8+} ion was given a softness value of 0 in the Ne row (note that *low B* values represent a *harder* ion).

With these assumptions, quadratic regression curves were successfully calculated for each isoelectronic row with correlation coefficients of above 0.99 (Fig. 1). These regression curves were used to evaluate B parameters for all remaining main-group elements. Unfortunately, there were not enough data points available in the literature for the He row. Thus, the ions B^{3+}, C^{4+} and N^{5+} could not be included in our calculations. However, $B(Be^{2+})$ was estimated using the observation that the ratios between the B parameters of alkaline earths over alkalis yield a nearly constant value of 0.76. Thus $B(Be^{2+})$ was extrapolated by multiplication of $B(Li^+)$ by 0.76.

In addition to the main-group elements, the first-row transition elements Ti^{4+}, Mn^{2+}, Fe^{2+}, Fe^{3+}, Co^{2+}, Ni^{2+}, Cu^{2+}, Zn^{2+} were included. For this purpose, the respective B parameters were assumed to be equal to $B(Ca^{2+})$ for transition metals with less

than five d electrons, and equal to $B(Ga^{3+})$ for five or more d electrons. This simplification for transition metals seems justified, since the effect of d valence electrons on the softness of a transition ion is not expected to follow a continuous trend. However, the repulsive effect of occupied e_g orbitals is incorporated in the change from $B(Ca^{2+})$ to $B(Ga^{3+})$ for transition metals with five or more d electrons. Furthermore, Lewis & Catlow (1985) showed that the even coarser approximation of taking the same ρ value for the whole row leads to reasonable λ's. The B values derived with the described procedure are given in Table 1.

Refinement of the A parameter

The crystal structures used to refine the Gilbert repulsion radii A_i are given in Table 1 with the corresponding ICSD codes obtained from the Inorganic Crystal Structure Database (Bergerhoff, Hundt, Sievers & Brown, 1983). Since van der Waals effects are, as mentioned above, not easy to handle, structure types with a distinct layer character and therefore significant van der Waals contributions were carefully avoided. The parameters were fitted to the structural arrangement using crystallographically independent cell parameters as well as atomic coordinates as observations. Gilbert radii A of Ti^{4+} and Al^{3+} were averaged from several structures. Since the scatter of the individual values was very small (0.03 and 0.02, respectively) only a single value was calculated for the other elements, even in cases where various possible structures were available.

Subsequently, the refined parameters were used for lattice-energy minimizations to model the structural arrangement which previously served as observations, where cell parameters and atomic coordinates were allowed to vary simultaneously. The largest deviations between these back-modeled and observed values are also given in Table 1. These deviations may seem rather large for some structures. However, it has to be kept in mind that the strongest deviations are in most cases caused by a single bond length.

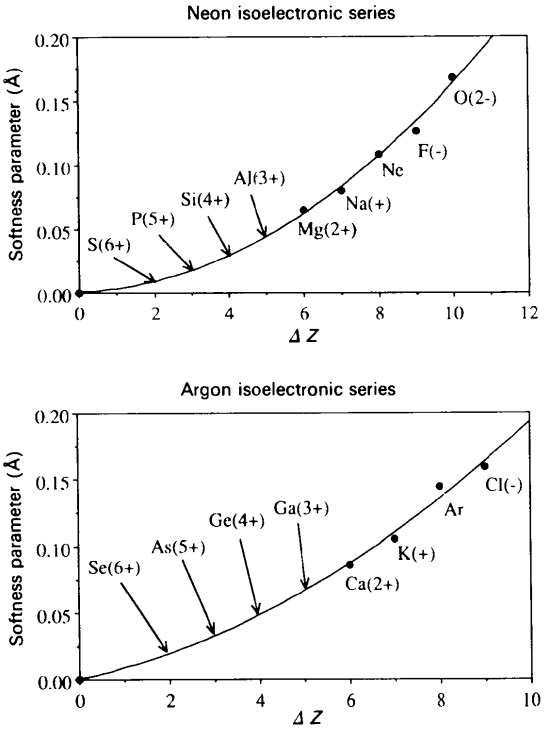

Fig. 1. Quadratic interpolation of softness parameters (B) for Ne and Ar isoelectronic series.

Table 1. *Values for A_i and B_i for various ions as determined from simple compounds*

Ion	Compound	Maximum deviation (%)	ICSD code	A_i (Å)	B_i (Å)
Li^+	Li_2O	0.0	22402	1.061	0.07
Na^+	Na_2O	0.0	60435	1.432	0.082
K^+	K_2O	0.0	60438	1.794	0.110
Rb^+	$RbAlO_2$	0.0	28373	1.967	0.119
Cs^+	$CsAlO_2$	0.0	28372	2.228	0.134
Be^{2+}	BeO	6.5	61181	0.875	0.053
Mg^{2+}	MgO	0.0	9863	1.243	0.062
Ca^{2+}	CaO	0.0	28905	1.597	0.086
Sr^{2+}	SrO	0.0	28904	1.758	0.091
Ba^{2+}	BaO	0.0	26961	1.953	0.101
Ti^{4+}	TiO_2 (rutile)	3.87	62677	1.485	0.086
	TiO_2 (anatase)	8.38	9852	1.503	
	TiO_2 (brookite)	1.74	36408	1.478	
	$CaTiSiO_5$	4.17	12131	1.480	
	$Ba_2TiSi_2O_8$	4.36	201844	1.513	
Ti^{2+}	TiO	0.0	60483	1.333	0.086
V^{2+}	VO	0.0	60486	1.276	0.086
Cr^{2+}	CrO	0.0	61633	1.293	0.086
Mn^{2+}	MnO	0.0	9864	1.366	0.066
Fe^{2+}	FeO	0.0	67197	1.335	0.066
Fe^{3+}	Fe_3O_4†	0.0	26410	1.400	0.066
Co^{2+}	CoO	0.0	9865	1.285	0.066
Ni^{2+}	NiO	0.0	9866	1.246	0.066
Cu^{2+}	CuO	0.0	61323	1.277	0.066
Zn^{2+}	ZnO	0.0	38222	1.293	0.066
Al^{3+}	Andalusite	2.24	24275	1.089	0.044
	Sillimanite	4.78	25711	1.120	
	Kyanite	2.4	16976	1.105	
Ga^{3+}	$LiGaO_2$	6.5	18152	1.329	0.066
In^{3+}	In_2O_3 (cubic)	0.69	14387	1.460	0.065
Si^{4+}	SiO_2 (α-quartz)	7.5	34644	1.008	0.029
Ge^{4+}	GeO_2	1.27	9182	1.199	0.048
Sn^{4+}	SnO_2	0.27	39173	1.314	0.045
Pb^{4+}	PbO_2	0.77	36250	1.425	0.049
P^{5+}	α-$AlPO_4$	2.09	30500	0.887	0.017
As^{5+}	α-$AlAsO_4$	6.2	33254	1.082	0.033
Sb^{5+}	Sb_2O_5	8.07	1422	1.268	0.028
Bi^{5+}	$BaBiO_3$	8.1	10319	1.417	0.030
O^{2-}	*Ab initio* calculation (Lasaga & Gibbs, 1987)			1.853	0.168
S^{6+}	$MgSO_4$	9.26	16759	0.865	0.009
Se^{6+}	Rb_2SeO_4		60928	1.085	0.019
Te^{6+}	Mg_3TeO_6	8.66	9089	1.219	0.015
F	LiF	0.0	62361	1.492	0.133
Cl	NaCl	0.0	100633	1.969	0.177
Br	KBr	0.0	22157	2.136	0.190
I	CsI	0.0	61517	2.238	0.215
He	Calculated from vibrational spectra by Gilbert (1968)			0.89	0.12
Ne	Calculated from vibrational spectra by Gilbert (1968)			1.1	0.109
Ar	Calculated from vibrational spectra by Gilbert (1968)			1.48	0.135

* Maximum deviation from the observed interatomic distance while back-refining structural parameters with the refined A value.

† For the refinement of $A(^{VI}Fe^{3+})$ with Fe_3O_4, the A parameters of $^{IV}Fe^{2+}$ and $^{VI}Fe^{3+}$ were refined simultaneously.

Bond lengths are very often sensitive to covalence effects (Lasaga & Gibbs, 1987). In the case of Si, which was refined with α-quartz, the back-modeling yielded a nearly perfect β-quartz structure leading to a maximum deviation of 7.5%. This is in agreement with the observation of previous studies (*e.g.* Lasaga & Gibbs, 1987) that a purely ionic model is not able to model the α-quartz structure, but will always lead to the β-quartz structure, since the structure of α-quartz is strongly stabilized by covalence effects. It may be argued that it is not reasonable to refine repulsion parameters with the structure of α-quartz as observation due to its covalent Si—O bonds. However, it has to be expected that the angle-bending covalence effects will not have much influence on the repulsion radii of the ions but rather on the bond angles due to three-body terms. Thus the hardness radii fitted from α-quartz may well have physically reasonable values though they are not able to model their 'source' structure within the framework of a two-body model. Control determinations of A_{Si} and B_{Si} with aluminosilicates and forsterite (Mg and Al values fixed to previously determined values) yielded similar results as obtained from the α-quartz refinement.

The determination of A values of the 6+ ions of the sixth group was affected by severe problems. Whereas refinement of repulsion radii for S^{6+} and Te^{6+} converged readily, the back-modeling yielded rather poor results. $A(Se^{6+})$ only converged with Rb_2SeO_4 (Takahashi, Onodera & Shiozaki, 1987) as a basis structure. However, back-modeling of the structural parameters with the determined A parameter was not possible. Least-squares calculations with structures of Li_2SeO_4 (Hartmann, 1989) and K_2SeO_4 (Kálmán, Stephens & Cruickshank, 1970) did not even converge to positive A values. This behavior when fitting ionic repulsion radii to cations of the sixth group may be understood in terms of the strong covalent double bonds which these ions are known to form (*e.g.* Kálmán, Stephens & Cruickshank, 1970). Since the assessment of the B parameter was based on the assumption of ionic potential interactions, a fit of the A values to structures with double bonds exhibiting extraordinarily short distances yields unreasonably low or even negative A parameters.

Comparison of repulsion parameters with chemical and physical properties

An inspection of Gilbert-type parameters A and B in terms of the periodic table of the elements yields a decreasing trend from left to right within a period for both parameters. In addition, both values show an increasing tendency from top to bottom of a group. Qualitatively identical trends within the periodic table are observed for the electronegativity and the Lewis acid strength (Brown, 1981), as well as for ionic radii as determined by Shannon (1976).

A closer look at these relations reveals a striking exponential correlation between the softness parameter B of the cations and the corresponding Lewis acid strengths (Fig. 2). Lewis acid strengths are defined by Brown (1981) as the quotient of the formal ionic charge over the average coordination number of the ion (determined as the average of all known compounds). Thus the Lewis acid strength can be visualized as a measure of the strength of a bond typically formed by a particular cation. Fig. 2 shows that ions with low B values *i.e.* 'hard' ions have high Lewis acid strengths. This relationship seems physically reasonable since cations of higher periods with high oxidation states (which have low B values in our assumption) are known to behave more rigidly with respect to their bonds than alkalis and alkaline earths do.

A remarkable parallelism can also be observed between the A parameters and the octahedral ionic radii given by Shannon (1976) (Fig. 3*a*), underlining the physical interpretation of A as a repulsion radius. Locally the A parameter even reflects subtle kinks within the ionic radii curve of certain groups. The absolute difference between repulsion radius and ionic radius increases with group number. This may be understood in terms of the increasing charge for higher groups within an isoelectronic row. A higher electrostatic charge requires a larger repulsion radius to keep the lattice stable. In addition, the A parameters show a nearly linear decrease with increasing Z (Z = atomic number) within an isoelectronic series, confirming assumption (3) of a linear decrease of the valence-shell radius with increasing Z.

The variation of A within the first-row transition metals is physically reasonable since it reflects the double minimum found for many first-row transition-metal properties (Orgel, 1961; Lewis & Catlow, 1985) (Fig. 3*b*).

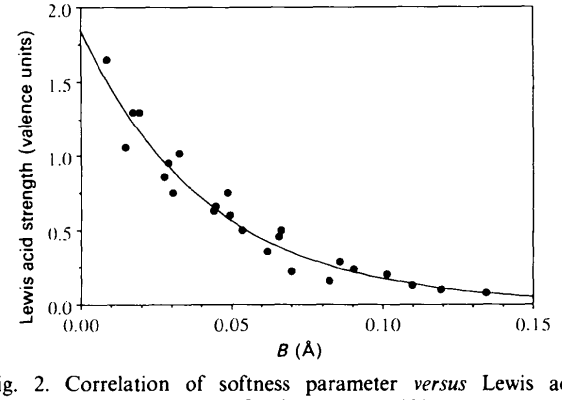

Fig. 2. Correlation of softness parameter *versus* Lewis acid strength as defined by Brown (1981).

Calculations of vibrational frequencies (Gramaccioli & Pilati, personal communication) based on our parameters yielded several imaginary frequencies indicating the limitations of our model in simulating physical properties. Since the repulsion parameters determined in this work have been adjusted to static lattice energies, they cannot be expected to predict quantities which are related to dynamic terms.

Extrapolation of repulsion radii

The striking parallelism between the repulsion radius A and the octahedral ionic radius encourages efforts to find a way of roughly estimating the repulsion radius of any desired ion. This would be especially helpful for ions with a charge lower than the maximum oxidation state, where the procedure of determining the softness parameter B and subsequent refinement of the repulsion radius A cannot be applied. In these cases, the repulsion parameter A may be determined on the basis of the octahedral ionic radius (Shannon, 1976). Having determined A by this approach, the softness parameter B can be refined, keeping the repulsion radius A fixed. Thus the repulsion radius A of a main-group ion is calculated as a sum of the form:

$$A = \mathrm{IR}^{\mathrm{VI}} + \Delta,$$

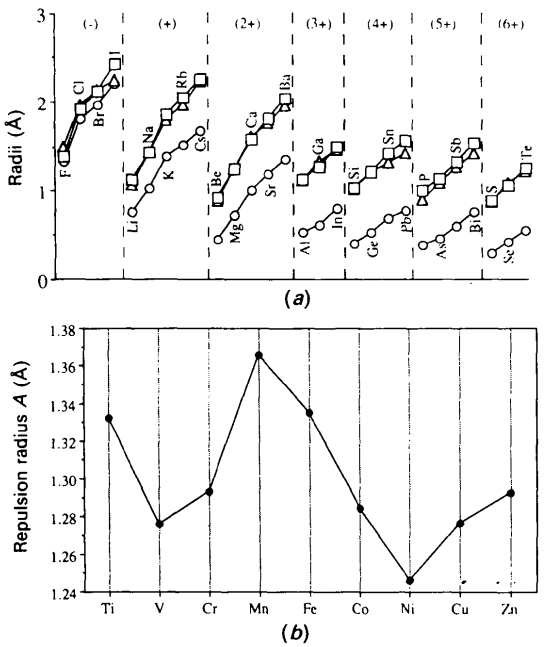

Fig. 3. (*a*) Comparison between octahedral ionic radii (circles), refined repulsion radii (triangles) and modeled repulsion radii (squares) of main-group ions. Atoms within main groups are connected with a solid line. (*b*) Repulsion radii of divalent first-row transition metals. Note the two minima at V^{2+} and Ni^{2+}, which are also reflected in various physical and chemical properties (Orgel, 1961).

where $\mathrm{IR}^{\mathrm{VI}}$ represents the octahedral ionic radius and Δ is a function of the formal charge of the ion as well as the period number.

A close examination of the difference between repulsion radii and the respective octahedral ionic radii (Fig. 3*a*) reveals, as mentioned above, a nearly linear increase within a group (say constant charge) with increasing period and – within the range of interest – a quadratic relationship within a period. The two relationships are assumed to be independent and can therefore be approximated by fitting a quadratic regression line through the difference radii as a function of the formal charge (Δ_{charge}) and a linear regression line through the difference radii as a function of the period (Δ_{period}). For the assessment of Δ_{charge}, we chose the ions of the fourth period. The difference radii of the fourth period are plotted against the formal charge and a quadratic regression curve of the form

$$\Delta_{\mathrm{charge}} = 0.33544 + 0.15542 \times \mathrm{charge} - 0.0175 \times (\mathrm{charge})^2$$

was fitted through the data points ($R^2 = 0.945$).

A linear regression line with the parameters

$$\Delta_{\mathrm{period}} = 0.26136 + 0.055(p - 4)$$

was calculated through the difference radii of the first group ($R^2 = 0.89$), where p stands for the period number. The variable is chosen as $(p - 4)$ since the quadratic charge dependence was established for the fourth period. The two functions are combined linearly by simple addition yielding the function:

$$A = \mathrm{IR}^{\mathrm{VI}} + 0.5968 + 0.1544 \times (\mathrm{charge}) - 0.0175 \times (\mathrm{charge})^2 + 0.055(p - 4).$$

Fig. 3(*a*) shows a comparison between the refined repulsion radii A and the A parameters as calculated on the basis of the octahedral ionic radius. The agreement between the two values is encouraging.

Reliability of the repulsion parameters

In spite of all the correlations between repulsion parameters and physical values, the only way to determine the reliability of the parameters is to test their ability to model structures. Interesting examples for this purpose are compounds of the Mg—Si—O system, since a lot of modeling with various repulsion parameters and methods has been done on this system (Miyamoto & Takeda, 1980, 1984; Price & Parker, 1984; Matsui & Busing, 1984; Matsui, 1988; Kubicki & Lasaga, 1991). An extensive compilation of Mg-silicate structure simulations is given by Miyamoto & Takeda (1984). This set of structure simulations seems to be ideal for comparison with our data due to its consistency with regard to the repul-

sion models applied. The authors fixed Gilbert-type parameters of Mg^{2+} (A_{Mg}, B_{Mg}) to the values determined by Busing (1970) and then subsequently simultaneously fitted A and B for Si^{4+} and O^{2-} to the structure of α-Mg_2SiO_4. With these results, they simulated the structures of α-Mg_2SiO_4, β-Mg_2SiO_4, γ-Mg_2SiO_4, $MgSiO_3$ (perovskite) and $MgSiO_3$ (ilmenite).

Table 2 shows a comparison of their data with our results: it is evident from Table 2 that for all Mg_2SiO_4 modifications, the results of Miyamoto & Takeda (1984) are slightly superior to our data. This was expected, since their repulsion potential was adjusted to the forsterite structure, which is very similar to the subsequently simulated Mg_2SiO_4 polymorphs. However, in those two cases where the stoichiometry of the structure in question deviates from the forsterite stoichiometry (perovskite and ilmenite), our repulsion parameters model the observed structural arrangement even better.

These examples demonstrate that a repulsion model derived from extrapolated B values and A values fitted to simple binary oxides does not predict structures as accurately as repulsion parameters derived directly from identical or very similar structure types. However, the transferability of the parameters to different structure types is very encouraging.

Table 2. *Comparison of observed cell dimensions and interatomic distances with those obtained by structure simulations (all quantities are given in* Å)

Numbers in parentheses represent the percentage deviation from the observed value. Observed values from: (*a*) Smyth & Hazen (1973); (*b*) Horiuchi & Sawamoto (1981); (*c*) Sasaki, Prewitt, Sato & Ito (1982); (*d*) Matsui (1982); (*e*) Horiuchi, Hirano, Ito & Matsui (1982).

Variable	This work	Miyamoto & Takeda (1984)	Observed
α-Mg_2SiO_4 (forsterite)[a]			
a	4.955 (4.2)	4.799 (0.9)	4.756
b	10.281 (0.7)	10.141 (0.6)	10.207
c	6.036 (0.9)	5.911 (1.2)	5.98
Si—O(1)	1.616 (0.1)	1.623 (0.5)	1.615
Si—O(2)	1.644 (0.5)	1.660 (0.4)	1.653
Si—O(3) (2 ×)	1.625 (0.6)	1.634 (0.1)	1.635
Mg(1)—O(1) (2 ×)	2.093 (0.4)	2.037 (2.3)	2.085
Mg(1)—O(2) (2 ×)	2.159 (4.4)	2.088 (0.9)	2.068
Mg(1)—O(3) (2 ×)	2.217 (4.3)	2.165 (1.5)	2.132
Mg(2)—O(1)	2.221 (1.8)	2.207 (1.1)	2.182
Mg(2)—O(2)	2.106 (2.7)	2.042 (0.4)	2.051
Mg(2)—O(3) (2 ×)	2.073 (0.3)	1.971 (4.6)	2.067
Mg(2)—O(3) (2 ×)	2.332 (5.3)	2.299 (3.8)	2.214
β-Mg_2SiO_4[b]			
a	5.812 (2.0)	5.686 (0.2)	5.698
b	11.690 (2.2)	11.452 (0.1)	11.438
c	8.340 (1.0)	8.182 (0.9)	8.257
Si—O(2)	1.680 (1.2)	1.676 (1.5)	1.701
Si—O(3)	1.632 (0.4)	1.637 (0.1)	1.638
Si—O(4) (2 ×)	1.633 (0.1)	1.642 (0.7)	1.632
Mg(1)—O(3) (2 ×)	2.172 (2.7)	2.108 (0.3)	2.115
Mg(1)—O(4) (2 ×)	2.095 (2.4)	2.042 (0.2)	2.046
Mg(2)—O(1)	2.007 (1.4)	1.955 (3.9)	2.035
Mg(2)—O(2)	2.310 (10.3)	2.251 (7.4)	2.095
Mg(2)—O(4) (2 ×)	2.146 (2.5)	2.076 (0.8)	2.093
Mg(3)—O(1) (2 ×)	2.051 (1.7)	1.999 (0.9)	2.016
Mg(3)—O(3) (2 ×)	2.169 (2.2)	2.112 (0.5)	2.123
Mg(3)—O(4) (2 ×)	2.197 (3.2)	2.112 (0.8)	2.129
γ-Mg_2SiO_4 (spinel)[c]			
a	8.188 (1.5)	8.042 (0.3)	8.065
Si—O (4 ×)	1.652 (0.2)	1.653 (0.1)	1.655
Mg—O (6 ×)	2.119 (2.4)	2.063 (0.3)	2.070
$MgSiO_3$ (perovskite)[d]			
a	4.832 (1.2)	4.848 (1.5)	4.775
b	4.965 (0.7)	5.032 (2.1)	4.929
c	6.927 (0.4)	7.097 (2.9)	6.897
Si—O(1) (2 ×)	1.772 (0.6)	1.851 (3.6)	1.783
Si—O(2) (2 ×)	1.773 (1.3)	1.820 (1.6)	1.796
Si—O(2) (2 ×)	1.777 (1.3)	1.819 (1.1)	1.800
Mg—O(1)	2.076 (3.1)	1.977 (4.8)	2.014
Mg—O(1)	2.148 (2.4)	2.319 (10.6)	2.097
Mg—O(2) (2 ×)	2.208 (7.6)	2.030 (1.1)	2.052
Mg—O(2) (2 ×)	2.278 (0.6)	2.421 (5.6)	2.292
Mg—O(2) (2 ×)	2.403 (1.0)	2.531 (4.2)	2.427
$MgSiO_3$ (ilmenite)[e]			
a	4.836 (2.3)	4.797 (1.5)	4.728
c	13.255 (2.2)	13.735 (1.3)	13.559
Si—O (3 ×)	1.780 (0.7)	1.700 (3.8)	1.768
Si—O (3 ×)	1.853 (1.3)	2.012 (9.9)	1.830
Mg—O (3 ×)	2.004 (0.7)	1.995 (0.3)	1.989
Mg—O (3 ×)	2.169 (0.2)	2.190 (1.2)	2.163

Simulation of corundum- and ilmenite-type structures

As a further test of the reliability of the new set of repulsive potentials, we applied them to compounds with corundum or ilmenite structure. These structure types are especially suitable for such an experiment, since they are known to exhibit a strong out-of-center distortion of the octahedral cations due to ionic repulsion across face-sharing octahedra. The extent of this distortion for main-group element compounds is determined by the cation–cation Coulomb repulsion as well as by the cation–anion short-range repulsion, *i.e.* for a given anion species the cation repulsion radius and ionic softness. Since the repulsion radius is, as shown above, strongly correlated with the ionic radius (Fig. 3*a*), the extent of the out-of-center shift is expected to correlate with the size of the cation relative to its site size. This can be easily tested by comparing the out-of-center shift with the difference between octahedral size and cation diameter. The octahedral size in corundum-like structures can be defined as $c/6$, since six face-sharing octahedral sites define the length of the c axis. Fig. 4 shows a plot of the difference between octahedral size ($=c/6$) minus cation diameter [ionic radii from Shannon (1976)] *versus* out-of-center shift for the main-group element compounds Al_2O_3, Ga_2O_3 and In_2O_3. The model implies that for the case where the difference between octahedral size and cation size becomes zero, the out-of-centre shift should also be zero. Thus, the origin is included in a linear-regression analysis. The correlation coefficient of this regression curve is 0.997 (Fig. 4).

A different situation is found in corundum- and ilmenite-type structures formed by transition metals. In these cases, the off-center shift caused primarily by electrostatic repulsion is strongly modified by metal–metal interactions (Goodenough, 1963, 1965), which are clearly absent in main-group compounds

(Lewis, Schwarzenbach & Flack, 1982). Thus, Ti_2O_3, exhibiting significant metal–metal bonds along c (Vincent, Yvon, Grüttner & Ashkenazi, 1980; Rice & Robinson, 1977; Prewitt, Shannon, Rogers & Sleight, 1969), reveals a suspiciously short out-of-center distance (0.15 Å), whereas hematite (Fe_2O_3), despite having a c axis very similar to Ti_2O_3, shows one of the strongest out-of-center shifts (0.3 Å) found in corundum-type structures. This is explained by missing metal–metal interactions along c (Goodenough, 1963, 1965) as well as filled e_g orbitals, which widen the mean bond length (Goodenough, 1963, 1965; Tossell, Vaughan & Johnson, 1973), thus leaving more space for out-of-center distortions in hematite.

V_2O_3 exhibits metal–metal bonds across the common edge, *i.e.* parallel to the a axis (Vincent, Yvon & Ashkenazi, 1980; Prewitt, Shannon, Rogers & Sleight, 1968). However, since metal–metal bonds along c are lacking at room temperature (Vincent, Yvon & Ashkenazi, 1980), the out-of-center shift is not shortened to the extent observed in Ti_2O_3.

Cr_2O_3, despite having metal–metal interactions along c similar to Ti_2O_3, has an out-of-center shift which is even slightly larger than in V_2O_3. This may be explained by the smaller ionic radius of Cr^{3+} compared to Ti^{3+} and V^{3+}, which is correlated with a smaller repulsion radius. This effect partly balances the metal–metal contraction along c.

Structure simulations of hematite (Fe_2O_3) are strongly affected by problems inherent to transition elements as mentioned above. For the case of Ti_2O_3, the energy minimization did not even converge to a reasonable solution.

Table 3 shows the results of some corundum- and ilmenite-type structure simulations. It is obvious that main-group element structures can be modeled with much more accuracy than transition-element structures. In fact, predictions of corundum-type structures of main-group elements (Al_2O_3, Ga_2O_3, In_2O_3) agree very well with the observed structural arrangement. The high relative deviation of the cation off-center shift (between 2.5 and 10%) may be explained by the fact that only cell parameters and coordinates (*i.e.* bond lengths) are used as variables for the energy minimization. Thus a relatively small error in these values may induce a relatively high deviation in the much smaller scale out-of-center shift. On the absolute scale, these deviations are within some hundredths or thousandths of an ångström (between 0.007 and 0.03 Å).

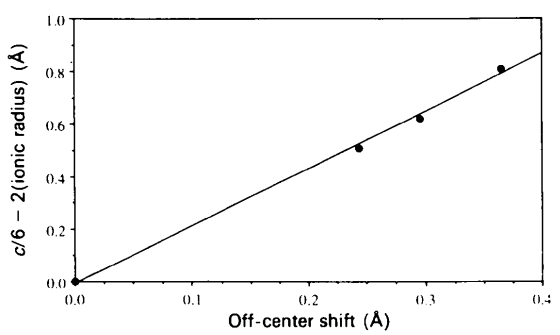

Fig. 4. Plot of octahedral space [$= c/6 - 2$(ionic radius)] *versus* off-center shift of main-group-element corundum-type compounds.

Table 3. *Comparison of observed and calculated corundum- and ilmenite-type structures*

All cations at (0,0,z). Oxygens of corundum-type structures at (x,0,$\frac{1}{4}$). Observed values from: (*a*) Cox, Moodenbaugh, Sleight & Chen (1980); (*b*) Marezio & Remeika (1967); (*c*) Prewitt, Shannon, Rogers & Sleight (1969); (*d*) Antipin, Tzirelson, Flugge, Gerr, Struchkov & Ozerov (1985); (*e*) Wechsler & von Dreele (1989); (*f*) Kidoh, Tanaka, Marumo & Takei (1984); (*g*) Kidoh, Tanaka & Marumo (1984); (*h*) Wechsler & Prewitt (1984).

	Al_2O_3[a]	Ga_2O_3[b]	In_2O_3[c]	Fe_2O_3[d]
a_{obs} (Å)	4.7640 (1)	4.9825 (5)	5.4870 (3)	5.0342 (3)
a_{calc} (Å)	4.7673	5.0273	5.4398	5.2798
c_{obs} (Å)	13.0091 (1)	13.433 (3)	14.510 (1)	13.7483 (4)
c_{calc} (Å)	12.9023	13.466	14.453	14.1235
$M(z)_{obs}$	0.35221 (8)	0.3554 (2)	0.35731 (2)	0.3553 (1)
$M(z)_{calc}$	0.35404	0.3548	0.35479	0.3545
$O(x)_{obs}$	0.30636 (8)	0.3049 (3)	0.2980 (5)	0.6942 (1)
$O(x)_{calc}$	0.30128	0.2986	0.2952	0.7026
Average absolute deviation of cation–anion distances (Å)	0.0044	0.0257	0.0286	0.0782

	$MgTiO_3$[e]	$CoTiO_3$[f]	$MnTiO_3$[g]	$FeTiO_3$[h]
a_{obs} (Å)	5.0548 (3)	5.0662 (2)	5.13948 (5)	5.0884 (1)
a_{calc} (Å)	5.1544	5.1718	5.23290	5.2101
c_{obs} (Å)	13.8992 (7)	13.918 (3)	14.2829 (4)	14.0855 (4)
c_{calc} (Å)	13.9018	14.014	14.4427	14.2726
$M(z)_{obs}$	0.35570 (5)	0.35511 (1)	0.36002 (1)	0.35537 (2)
$M(z)_{calc}$	0.36151	0.36182	0.36151	0.36159
$Ti(z)_{obs}$	0.14510 (7)	0.14558 (1)	0.14758 (1)	0.14640 (2)
$Ti(z)_{calc}$	0.15150	0.15207	0.15384	0.15314
$O(x)_{obs}$	0.31591 (8)	0.31623 (8)	0.3189 (1)	0.3174 (2)
$O(x)_{calc}$	0.31201	0.31279	0.3152	0.3143
$O(y)_{obs}$	0.02146 (8)	0.02091 (8)	0.0310 (1)	0.0233 (2)
$O(y)_{calc}$	0.02512	0.02717	0.0355	0.0324
$O(z)_{obs}$	0.24635 (3)	0.24588 (3)	0.24393 (3)	0.24506 (5)
$O(z)_{calc}$	0.24025	0.23966	0.23773	0.23848
Average absolute deviation of cation–anion distances (Å)	0.0822	0.0881	0.0774	0.0974

With the ilmenite structures, the best result is again found for a structure consisting of main-group elements only ($MgSiO_3$) (see Table 2). Nevertheless, four examples with transition elements have been calculated. As can be seen from Table 3, the structure simulation of these compounds did not achieve the accuracy found for the main-group compounds. However, the structural features of the compounds are approximately predicted, though some individual values show poor agreement. The modeling of the off-center shift failed for these examples. In particular the Ti value is always underestimated, whereas the off-center shift of the other ion is overestimated in all four cases.

Modeling of some Ti-containing compounds

The new repulsion parameters were also applied to some more complicated Ti compounds. In particular,

an attempt was made to reproduce distortions of the octahedral Ti coordinations. For this purpose, the crystal structures of titanite ($CaTiSiO_5$) (Speer & Gibbs, 1976), fresnoite ($Ba_2TiSi_2O_8$) (Markgraf, Halliyal, Bhalla, Newnham & Prewitt, 1985) and neptunite ($KNa_2LiTi_2Fe_2Si_8O_{24}$) (Kunz, Armbruster, Lager, Schultz, Goyette, Lottermoser & Amthauer, 1991) were refined by energy minimization with the program *WMIN*. Because of the structural and chemical complexity of neptunite (40 atoms per asymmetric unit), only cell parameters and the transition-metal positions were refined for this example.

Table 4 gives the results of these computer simulations. At a first glance the agreement of the modeled structure with the observed value is not very good. Closer examination of Table 4 reveals that for titanite all cations as well as O1 are placed in pseudo-special positions. This yields quite reasonable Si—O bonds (average deviation 0.7 and 0.3% respectively), but rather high deviations for the soft Ca—O bonds and for the short Ti—O bonds. The position of the Ti atom is modeled in the center of a distorted octahedral environment in contradiction to the observed arrangement. Fresnoite shows the largest deviations around the weakly bonded Ba site. For fresnoite as well as for neptunite the geometric pattern around the Ti atom is predicted correctly in a qualitative sense.

To evaluate the possible influence of neglecting the van der Waals terms, we started a *WMIN* run for fresnoite, including an isotropic dispersion term. These terms include a constant D_{ij}, which is calculated after Margenau (1939) from ionization energy and electronic polarizability. The D constants for fresnoite were evaluated taking the ionization energies from Francis (1960) and the electronic polarizabilities from Lasaga & Cygan (1982). The Ba—O bond lengths were reproduced slightly better with this model. In addition, cell parameters were superior to those of the model without any van der Waals term. The distorted Ti coordination could not be simulated with satisfactory accuracy.

An alternative approach to modeling out-of-center distortions

An approach which is detached from any problems concerning covalence and polarizability is the bond-valence model (*e.g.* Brown, 1981). This model makes no assumptions regarding the physical nature of the bond and its validity does not depend on the ionicity or covalence of a bond. The method is based on the empirical observation that the valence of an atom can be distributed between the bonds it forms and that the resultant bond valences correlate with bond

Table 4. *Simulations of various* Ti *compounds*

Observed values from: (*a*) Speer & Gibbs (1976); (*b*) Markgraf, Halliyal, Bhalla, Newnham & Prewitt (1985); (*c*) Kunz, Armbruster, Lager, Schultz, Goyette, Lottermoser & Amthauer (1991).

$CaTiSiO_5$ (titanite)[a]

Variable	Observed cell	Calculated cell	Difference (%)
a (Å)	7.069 (2)	7.278	2.9
b (Å)	8.722 (5)	8.856	1.5
c (Å)	6.566 (8)	6.858	4.4
β (°)	113.86 (2)	115.75	1.7

	Observed fractional coordinates			Calculated fractional coordinates		
Site	*x*	*y*	*z*	*x*	*y*	*z*
Ca	0.2424 (2)	0.9184 (1)	0.7512 (1)	0.2500	0.9318	0.7500
Ti	0.5134 (1)	0.7542 (1)	0.2495 (1)	0.5000	0.7500	0.2500
Si	0.7486 (2)	0.9330 (1)	0.7490 (2)	0.7500	0.9271	0.7500
O1	0.7499 (6)	0.8202 (4)	0.2502 (7)	0.7500	0.8090	0.2500
O2	0.9108 (6)	0.8162 (6)	0.9347 (6)	0.8846	0.8101	0.9431
O3	0.3827 (5)	0.9608 (4)	0.1459 (6)	0.3946	0.9637	0.1824
O4	0.9122 (6)	0.3165 (4)	0.4368 (6)	0.8846	0.3101	0.4431
O5	0.3813 (5)	0.4601 (4)	0.6468 (6)	0.3946	0.4637	0.6824

Average absolute deviation of cation–anion distances = 0.10 Å

$Ba_2TiSi_2O_8$ (fresnoite)[b] (without van der Waals term)

Variable	Observed cell	Calculated cell	Difference (%)
a (Å)	8.527 (1)	8.642	1.4
c (Å)	5.210 (9)	5.630	8.0

	Observed fractional coordinates			Calculated fractional coordinates		
Site	*x*	*y*	*z*	*x*	*y*	*z*
Ba	0.32701 (3)	0.82701 (3)	0	0.32583	0.82583	0
Ti	0	0	−0.5354 (5)	0	0	−0.5363
Si	0.128 (2)	0.628 (2)	−0.5129 (8)	0.129	0.629	−0.5044
O1	0	½	−0.629 (2)	0	½	−0.592
O2	0.1259 (5)	0.6259 (5)	−0.205 (1)	0.1257	0.6257	−0.220
O3	0.2924 (6)	0.5772 (8)	−0.643 (1)	0.2981	0.5810	−0.606
O4	0	0	−0.210 (2)	0	0	−0.218

Average absolute deviation of cation–anion distances = 0.11 Å

$Ba_2TiSi_2O_8$ (fresnoite)[b] (with van der Waals term)

Variable	Observed cell	Calculated cell	Difference (%)
a (Å)	8.527	8.588	0.7
c (Å)	5.210	5.464	4.9

	Observed fractional coordinates			Calculated fractional coordinates		
Site	*x*	*y*	*z*	*x*	*y*	*z*
Ba	0.32701 (3)	0.82701 (3)	0	0.32625	0.82625	0
Ti	0	0	−0.5354 (5)	0	0	−0.5426
Si	0.128 (2)	0.628 (2)	−0.5129 (8)	0.129	0.629	−0.5071
O1	0	½	−0.629 (2)	0	½	−0.597
O2	0.1259 (5)	0.6259 (5)	−0.205 (1)	0.1251	0.6251	−0.215
O3	0.2924 (6)	0.5772 (8)	−0.643 (1)	0.2987	0.5819	−0.611
O4	0	0	−0.210 (2)	0	0	−0.215

Average absolute deviation of cation–anion distances = 0.09 Å

$LiNa_2KTi_2Fe_2Si_8O_{24}$ (neptunite)[c]

Variable	Observed cell	Calculated cell	Difference (%)
a (Å)	16.430 (3)	16.893	2.9
b (Å)	12.436 (2)	12.407	1.5
c (Å)	9.963 (2)	10.117	4.4
β (°)	115.60 (1)	115.94	1.7

	Observed fractional coordinates			Calculated fractional coordinates		
Site	*x*	*y*	*z*	*x*	*y*	*z*
Ti1	0.3419 (1)	0.32516 (7)	0.1032 (2)	0.3378	0.31874	0.0869
Fe1	−0.3384 (1)	−0.31636 (7)	−0.0959 (2)	−0.3366	−0.32215	−0.1021
Ti2	0.0876 (2)	0.05251 (7)	0.1141 (2)	0.0870	0.05924	0.1001
Fe2	−0.0886 (1)	−0.06083 (7)	−0.1116 (2)	−0.0900	−0.05572	−0.1171

Average absolute deviation of (Fe,Ti)–oxygen distances = 0.07 Å

lengths. Brown & Altermatt (1985) found the widely used parameterization of the bond-valence–bond-length dependence, using a version of the exponential form originally proposed by Pauling (1947): $s_{ij} = \exp(R_0 - R_{ij})/0.37)$, where s_{ij} is the bond valence of bond-connecting ions i and j, R_0 is a bond-specific constant, and R_{ij} is the bond length between ions i and j. The bond-specific constants R_0 are derived by fitting the expression to a large number of known structures.

In addition to this definition there is the requirement that in a stable structure, the sum of all bond valences at any ion must be, as nearly as possible, equal to the formal charge of the respective ion. This rule, known as the valence sum rule, and the exponential form of the bond-valence–bond-length function lead to the distortion theorem as stated by Brown & Shannon (1973): *In any coordination sphere in which the averge bond length is kept constant, any deviation of the individual bond lengths from this value will increase the valence sum at the central atom.*

This means that an atom which is undersaturated in terms of the bond-valence model, *i.e.* the sum of all bond valences at this atom is lower than its formal charge, may raise this bond-valence sum by an out-of-center distortion, in which individual bond lengths deviate from an average value which is kept constant.

In the case of neptunite, we find iron and titanium to be ordered onto a total of four crystallographically distinct octahedral sites, where the Fe octahedra and Ti octahedra show striking differences in their distortions (Kunz, Armbruster, Lager, Schultz, Goyette, Lottermoser & Amthauer, 1991). Taking the two Ti sites, we find the bond-valence sum for the central atom to be about 3.7 when the cation is placed at the geometric center of the octahedron. Thus, Ti^{4+} in neptunite is underbonded if placed at the geometric octahedral center. According to the distortion theorem cited above, the bond-valence sum increases if the Ti atom is placed out-of-center within the coordination sphere. However, the direction the off-center shift will go is not discernible from this point of view. For this purpose the bond-valence sums of the surrounding oxygens have to be taken into consideration. Examination of the oxygen bond-valence sums reveals large variations between about 1.1 and 2.2 when the cation is placed at the geometric center. Thus, some O atoms seem to be strongly underbonded whereas others are considerably overbonded. We assume therefore that a possible out-of-center shift will be directed towards the oxygens with low bond-valence sums and away from those with bond-valence sums higher than 2.0, thus simultaneously relaxing cation undersaturation and unbalanced oxygen valence sums.

To determine the ideal Ti^{4+} position suggested by the bond-valence model, we refined the Ti^{4+} position within its octahedral surrounding with the constraint that oxygen valence sums were forced to be as equal as possible. With a self-written program, the test function $R = \sum[(V_m - V_i)/V_m]$ (V_m is the mean valence sum averaged over six oxygens, V_i are individual oxygen valence sums) is minimized as a function of the polar coordinates (ρ, Ω, φ) of the central metal atom. The polar coordinates for each oxygen octahedron were calculated with respect to the geometric center representing the origin using conformational data and the program *EUCLID* (Essén, 1983).

As can be seen from Table 5(*a*), the Ti positions modeled by this method show fair agreement with the observed position. However, the off-center shift is slightly overestimated by about 0.05 Å and the deviation of the calculated shift vector from the observed one lies within 13°. The variation of the oxygen valence sums for the modeled position is set within narrow ranges (1.87–1.94, 1.89–1.96 respectively). In addition the valence sum of the Ti^{4+} ions is increased to 3.96 and 3.95 for Ti(1) and Ti(2), respectively. However, the range of the observed oxygen valence sums is wider (1.69–2.14 and 1.61–2.10, respectively) and the observed Ti^{4+} valence sums of 3.83 and 3.84 are lower than the calculated values.

There are two explanations for the limited accuracy of the proposed model:

(1) Our model treats each octahedron as isolated from its crysallographic surroundings. Thus feedback effects of the shifting central metal on its neighbouring cations are not considered and may lead to errors.

(2) Point (1) cannot explain the deviation of the observed valence sums from their ideal values. This might be caused by basic limitations concerning the accuracy of this model. The empirical nature of the ion-specific constant (R_0) being fitted to many structure types may lead to slight deviations in the calculated bond-valence sum from the formal charge for an individual structure.

Nevertheless the agreement of the Ti^{4+} shift with respect to size and direction as modeled using the bond-valence model, is considerably better in a qualitative and quantitative sense than Ti^{4+} sites calculated with the ionic potential approach (Table 5*b*).

The bond-valence concept is not applicable to the Fe^{2+} sites in neptunite. We have two possible explanations for this failure:

(1) As can be seen from Table 5(*a*), bond-valence sums of the two Fe^{2+} sites are high (2.2) even if the Fe atoms were placed at the geometric center. Thus according to the distortion theorem, any possible out-of-center shift due to undersaturated ligands

Table 5. *Geometric data for neptunite*

Numbers in parentheses refer to the last digit and indicate the standard deviation.

(*a*) Cation and oxygen bond-valence sums and bond distances of neptunite metal octahedra

	Geometric center	Observed position	Bond-valence optimum
Ti(1)			
Bond-valence sums (valence units)			
O(4)	1.161	1.690	1.934
O(7)	1.950	2.077	1.923
O(7*a*)	2.132	2.002	1.874
O(10)	1.685	1.879	1.938
O(5*a*)	2.154	2.138	1.966
O(2)	1.993	2.016	1.927
Ti(1)	3.70	3.84	3.96
Interatomic distances (Å)			
O(4)	1.908	1.710 (4)	1.655
O(7)	2.018	1.997 (6)	2.035
O(7*a*)	1.988	2.187 (5)	2.254
O(10)	2.022	1.955 (4)	1.870
O(5*a*)	2.017	2.112 (5)	2.209
O(2)	1.984	2.039 (7)	2.032
Off-center shift	Δ angle = 13°	0.25 Å	0.31 Å
Ti(2)			
Bond-valence sums (valence units)			
O(1)	1.998	2.101	1.924
O(2*a*)	2.181	2.043	1.905
O(3)	1.675	1.882	1.906
O(4*a*)	1.096	1.612	1.917
O(5)	1.995	2.036	1.961
O(1*a*)	2.105	2.070	1.888
Ti(2)	3.71	3.83	3.94
Interatomic distances (Å)			
O(1)	1.972	1.969 (6)	2.205
O(2*a*)	1.990	2.200 (5)	2.288
O(3)	2.040	1.961 (4)	1.892
O(4*a*)	1.936	1.733 (5)	1.655
O(5)	2.011	2.056 (5)	2.037
O(1*a*)	1.976	2.071 (5)	2.162
Off-center shift	Δ angle = 11°	0.26 Å	0.33 Å

	Fe(1) Geometric center	Fe(1) Observed position		Fe(2) Geometric center	Fe(2) Observed position
Bond-valence sums (valence units)					
O(4*a*)	1.559	1.612	O(1)	2.253	2.100
O(10*a*)	1.698	2.070	O(2)	2.103	2.016
O(2*a*)	2.058	2.043	O(1*a*)	2.156	2.071
O(5)	2.134	2.036	O(3*a*)	1.721	1.882
O(7)	2.142	2.077	O(4)	1.629	1.690
O(7*a*)	2.014	2.002	O(5*a*)	2.074	2.137
Fe(1)	2.20	2.21	Fe(2)	2.27	2.23
Interatomic distances (Å)					
O(4*a*)	2.279	2.198 (4)	O(1)	2.011	2.153 (5)
O(10*a*)	2.075	1.968 (5)	O(2)	2.082	2.178 (5)
O(2*a*)	2.059	2.072 (7)	O(1*a*)	2.081	2.174 (6)
O(5)	2.086	2.196 (5)	O(3*a*)	2.100	1.971 (5)
O(7)	2.141	2.223 (5)	O(4)	2.277	2.187 (4)
O(7*a*)	2.103	2.115 (6)	O(5*a*)	2.136	2.072 (6)

(*b*) Ti and Fe off-center shift in neptunite: ionic model

	Observed (Å)	Calculated (Å)	Δ angle (°)*
Ti(1)	0.254	0.094	18.3
Ti(2)	0.258	0.111	20.4
Fe(1)	0.160	0.226	25.0
Fe(2)	0.180	0.225	19.1

* Δ angle = angle between observed and calculated shift vector, the geometric center taken as origin.

would increase the bond-valence sum of the cation and is therefore opposed by a tendency to maintain the bond lengths as regular as possible.

(2) Fe^{2+} (electron configuration $3d^6 4s^0$) occupies t_{2g} and e_g orbitals which are likely to form rigid π molecular orbitals in an octahedral surrounding (*e.g.* Gütlich, 1975), thereby stabilizing the central position of the Fe^{2+} ion.

Thus, the distortion of the Fe^{2+} octahedra in the neptunite structure represents a complex balance situation between a tendency to satisfy undersaturated oxygens and the requirement to maintain balanced bond lengths.

Despite these shortcomings, the bond-valence model can be used to understand the off-center distortion in fresnoite (Markgraf, Halliyal, Bhalla, Newnham & Prewitt, 1985). A Ti^{4+} ion hypothetically positioned at the geometric centre of its oxygen environment would exhibit a bond-valence sum of 3.7 and is therefore underbonded. At the observed out-of-center position, the Ti^{4+} ion has a bond-valence sum of 3.93. The *WMIN*-modeled Ti position is qualitatively similar to the observed arrangement where a short bond [Ti—O(4)] opposes four longer bonds [Ti—O(3)], but the extent of this distortion is underestimated in the ionic model. Nevertheless, the bond-valence sum calculated from the modeled position is 3.97, *i.e.* very close to the theoretical value of 4. It is not clear from this perspective why the observed out-of-center distortion is so strong, when similar bond-valence sums may be achieved with a smaller distortion. However, this may be understood by taking into account the average bond-valence sum of all O atoms. This value is clearly too low for Ti^{4+} at the central position (1.86). At the *WMIN*-modeled position, this value reaches 1.93, whereas the observed position leads to an average oxygen bond-valence sum of 1.98. The observed average is thus closest to the ideal value (2.0). This may be the cause of the high out-of-center shift, when compared with the arrangement produced by the ionic potential model.

The situation is even more subtle in the case of titanite ($CaTiSiO_5$; Speer & Gibbs, 1976). The bond-valence sum for Ti^{4+} at the geometric center is 3.92, which is very close to the formal charge of 4. However, for this case the oxgyen atom O(1) with formal

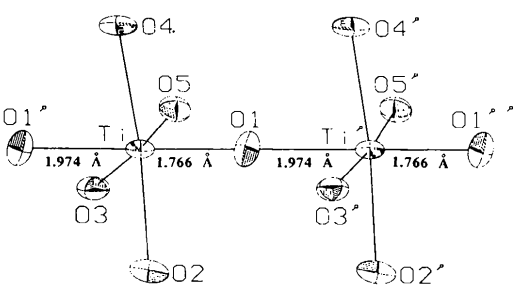

Fig. 5. Fragment of octahedral chain in titanite. Note the two non-equivalent bonds running from O(1) to two symmetric equivalent Ti atoms.

charge −2 has a bond-valence sum of only 1.69. Since Ti in titanite has two opposite bonds to O(1) (Fig. 5), there is the possibility of increasing the bond-valence sum of O(1) by an out-of-center distortion of the Ti ion in the direction of the O(1)—Ti—O(1) diameter. This out-of-center distortion increases the bond-valence sum of O(1) to a value of 2.1 thereby maintaining the bond-valence sum of Ti^{4+} at 4.09. Also the average oxygen bond valence is slightly increased to a value of 1.92, compared to 1.90 for a Ti position with six equal bonds. The ionic model, on the other hand, leads to a Ti bond-valence sum of 3.98 and an O(1) bond valence of 1.93. Both values are in good agreement with the formal charges of 4 and −2, respectively. However, the lowering of the average oxygen bond-valence sum to 1.86 in the modeled arrangement may be the reason that Ti in titanite displays off-center distortion, rather than the centric distortion suggested by the ionic model.

Concluding remarks

The consistent set of Gilbert-type repulsion parameters derived by quadratic extrapolation of the 'softness parameters' (B) onto isoelectronic species from Gilbert (1968) and fitting of the repulsion radii A to simple structures by energy minimization is able to simulate various crystal structures with an accuracy comparable to previous studies. In addition, these repulsion parameters seem to be able to model structures with various structure types and chemical compositions. Furthermore, the variation of repulsion radii (A) as well as softness parameters (B) within the periodic table shows reasonable correlations with chemical and physical properties.

However, the accuracy of a simple ionic model is limited by electronic effects leading to deformed coordination polyhedra. A simple approach based on the bond-valence model may lead to better results with respect to such covalence effects.

This work was supported by a grant of the Schweizerischer Nationalfonds, which is highly appreciated. The authors wish to thank Professor C. M. Gramaccioli and Dr T. Pilati for performing the vibrational-frequency calculations. Critical comments of the two referees helped to improve the manuscript. Larryn Diamond kindly corrected the English.

References

ANTIPIN, M. Y., TZIRELSON, V. G., FLUGGE, M. P., GERR, R. G., STRUCHKOV, Y. T. & OZEROV, R. P. (1985). *Dokl. Akad. Nauk SSSR*, **281**, 854–857.

BERGERHOFF, G., HUNDT, R., SIEVERS, R. & BROWN, I. D. (1983). *J. Chem. Inf. Comput. Sci.* **23**, 66–69.

BERTAUT, F. (1952). *J. Phys. Radium*, **13**, 499–505.

BORN, M. & MAYER, J. E. (1932). *Z. Phys.* **75**, 1–18.

BROWN, I. D. (1981). *Structure and Bonding*, edited by M. O'KEEFFE & A. NAVROTSKY, Vol. 2, pp. 1–30. New York: Academic Press.

BROWN, I. D. & ALTERMATT, D. (1985). *Acta Cryst.* B**41**, 244–247.

BROWN, I. D. & SHANNON, R. D. (1973). *Acta Cryst.* A**29**, 266–282.

BURNHAM, C. W. (1985). *Rev. Mineral.* **14**, 347–388.

BURNHAM, C. W. (1990). *Am. Mineral.* **75**, 443–463.

BUSING, W. R. (1970). *Trans. Am. Crystallogr. Assoc.* **6**, 57–69.

BUSING, W. R. (1981). *WMIN*. Report ORNL-5747. Oak Ridge National Laboratory, Tennessee, USA.

CATLOW, C. R. A. & PRICE, G. D. (1990). *Nature (London)*, **347**, 243–248.

COX, D. E., MOODENBAUGH, A. R., SLEIGHT, A. W. & CHEN, H. Y. (1980). *Natl Bur. Stand. (US) Spec. Publ.* **567**, 189–201.

DICK, B. G. & OVERHAUSER, A. W. (1958). *Phys. Rev.* **112**, 90–103.

ESSÉN, H. (1983). *J. Comput. Chem.* **4**, 136–141.

EWALD, P. P. (1921). *Ann. Phys.* **64**, 253–287.

FRANCIS, G. (1960). *Ionization Phenomena in Gases*, pp. 284–286. London: Butterworth.

GILBERT, T. L. (1968). *J. Chem. Phys.* **49**, 2640–2642.

GOODENOUGH, J. B. (1963). *Magnetism and the Chemical Bond*. New York: Interscience.

GOODENOUGH, J. B. (1965). *Bull. Soc. Chim. Fr.* **4**, 1200–1207.

GORDON, R. G. & KIM, Y. S. (1972). *J. Chem. Phys.* **56**, 3122–3133.

GÜTLICH, P. (1975). *Topics in Applied Physics*, edited by U. GONSER, Vol. 5, pp. 53–96. Heidelberg: Springer.

HARTMANN, P. (1989). *Z. Kristallogr.* **187**, 139–143.

HORIUCHI, H., HIRANO, M., ITO, E. & MATSUI, Y. (1982). *Am. Mineral.* **67**, 788–793.

HORIUCHI, H. & SAWAMOTO, H. (1981). *Am. Mineral.* **66**, 568–575.

KÁLMÁN, A., STEPHENS, J. S. & CRUICKSHANK, D. W. J. (1970). *Acta Cryst.* B**26**, 1451–1454.

KIDOH, K., TANAKA, K. & MARUMO, F. (1984). *Acta Cryst.* B**40**, 92–96.

KIDOH, K., TANAKA, K., MARUMO, F. & TAKEI, H. (1984). *Acta Cryst.* B**40**, 329–332.

KUBICKI, J. D. & LASAGA, A. C. (1991). *Phys. Chem. Miner.* **17**, 661–673.

KUNZ, M., ARMBRUSTER, T., LAGER, G., SCHULTZ, A. J., GOYETTE, R. J., LOTTERMOSER, W. & AMTHAUER, G. (1991). *Phys. Chem. Miner.* **18**, 199–213.

LASAGA, A. C. & CYGAN, R. T. (1982). *Am. Mineral.* **67**, 328–334.

LASAGA, A. C. & GIBBS, G. V. (1987). *Phys. Chem. Miner.* **14**, 107–117.

LASAGA, A. C. & GIBBS, G. V. (1988). *Phys. Chem. Miner.* **16**, 29–41.

LASAGA, A. C. & GIBBS, G. V. (1991). *Phys. Chem. Miner.* **17**, 485–491.

LEWIS, G. V. & CATLOW, C. R. A. (1985). *J. Phys. C*, **18**, 1149–1161.

LEWIS, J., SCHWARZENBACH, D. & FLACK, H. D. (1982). *Acta Cryst.* A**38**, 733–739.

MAREZIO, M. & REMEIKA, J. P. (1967). *J. Chem. Phys.* **46**, 1862–1865.

MARGENAU, H. (1939). *Rev. Mod. Phys.* **11**, 1–35.

MARKGRAF, S. A., HALLIYAL, A., BHALLA, A. S., NEWNHAM, R. E. & PREWITT, C. T. (1985). *Ferroelectrics*, **62**, 17–26.

MATSUI, M. (1988). *Phys. Chem. Miner.* **16**, 234–238.

MATSUI, M. & BUSING, W. R. (1984). *Phys. Chem. Miner.* **11**, 55–59.

MATSUI, Y. (1982). In *Collected Papers on The Materials Science of the Earth's Interior*, edited by I. SUNAGAWA & K. AOKI. The Japanese Association of Mineralogists, Petrologists and Economic Geologists, Tohoku Univ., Sendai, Japan.

MIYAMOTO, M. & TAKEDA, H. (1980). *Geochem. J.* **14**, 243–248.

MIYAMOTO, M. & TAKEDA, H. (1984). *Am. Mineral.* **69**, 711–718.
MULHAUSEN, C. & GORDON, R. G. (1981). *Phys. Rev. B*, **23**, 900–923.
ORGEL, L. E. (1961). *An Introduction to Transition Metal Chemistry: Ligand Field Theory*. London: Methuen.
PARKER, S. C. (1982). PhD thesis, Sir Christopher Ingold Laboratories, Univ. College, London.
PAULING, L. (1947). *J. Am. Chem. Soc.* **69**, 542–553.
POST, J. E. & BURNHAM, C. W. (1986). *Am. Mineral.* **71**, 142–150.
PREWITT, C. T., SHANNON, R. D., ROGERS, D. B. & SLEIGHT, A. W. (1969). *Inorg. Chem.* **8**, 1985–1993.
PRICE, G. D. & PARKER, S. C. (1984). *Phys. Chem. Miner.* **10**, 209–216.
RICE, C. E. & ROBINSON, W. R. (1977). *Acta Cryst.* B**33**, 1342–1348.
SASAKI, S., PREWITT, C. T., SATO, Y. & ITO, E. (1982). *J. Geophys. Res.* **87**, 7829–7832.
SHANNON, R. D. (1976). *Acta Cryst.* A**32**, 751–767.
SMYTH, J. R. & HAZEN, R. M. (1973). *Am. Mineral.* **58**, 588–593.
SPEER, J. A. & GIBBS, G. V. (1976). *Am. Mineral.* **61**, 238–247.
TAKAHASHI, I., ONODERA, A. & SHIOZAKI, Y. (1987). *Acta Cryst.* C**43**, 179–182.
TOSSELL, J. A., VAUGHAN, D. J. & JOHNSON, K. H. (1973). *Nature (London) Phys. Sci.* **244**, 42–45.
VINCENT, M. G., YVON, K. & ASHKENAZI, J. (1980). *Acta Cryst.* A**36**, 808–813.
VINCENT, M. G., YVON, K., GRÜTTNER, A. & ASHKENAZI, J. (1980). *Acta Cryst.* A**36**, 803–808.
WALDMANN, M. & GORDON, R. G. (1979). *J. Chem. Phys.* **71**, 1325–1329.
WECHSLER, B. A. & PREWITT, C. T. (1984). *Am. Mineral.* **69**, 176–185.
WECHSLER, B. A. & VON DREELE, R. B. (1989). *Acta Cryst.* B**45**, 542–549.

Acta Cryst. (1992). B**48**, 622–627

Calculated Intensities of Electron Waves Diffracted from Ti–14 wt% Mo Alloy Containing ω-Phase Crystals

BY M. AWAJI, H. HASHIMOTO, E. SUKEDAI AND F. AKAO

Faculty of Engineering, Okayama University of Science, Ridai-cho 1-1, *Okayama* 700, *Japan*

(*Received* 22 *January* 1991; *accepted* 6 *March* 1992)

Abstract

The amplitudes and intensities of electron waves diffracted from a Ti–14 wt% Mo alloy of β-phase containing ω-phase slabs of various thicknesses and at different depths were calculated. The intensities of the forbidden reflections $1/3\ \bar{1}2\bar{1}$, $2/3\ \bar{1}2\bar{1}$ and 121 from the ω_1-phase, which is one of the four variants of the ω-phase, are less than 1.0×10^{-5} even for a thickness of 40 Å. However, when an ω_1-phase of that thickness is included in a crystal of the β-phase at a depth of 80 Å, the intensity of the forbidden reflections increases to about 1.0×10^{-2} at the bottom surface of the ω_1-phase. The amplitudes of the $\bar{1}0\bar{1}$ and $2/3\ \bar{1}2\bar{1}$ waves are proportional to the distance of the ω_1-phase from the top surface and the thickness of that in the β-phase, respectively. When ω_1- and ω_2-phases overlap in the β-phase, extra spots such as $1/3\ \bar{1}0\bar{1}$, $2/3\ \bar{1}0\bar{1}$, 1/3 020 and 2/3 020 are excited at the top surface of the lower variant.

1. Introduction

Since the first observation of the ω-phase formed in aged Ti–Cr alloys (Frost, Parris, Hirsch, Doig & Schwartz, 1954), many studies using electron diffraction patterns and electron microscope images have been reported in other alloy systems (de Fontaine, Paton & Williams, 1971; Sass, 1972). Sukedai & Hashimoto (1989) showed that the projection of the ω_1- and ω_2-phases on the $(10\bar{1})$ plane has an ellipsoidal shape by taking the dark-field images from corresponding diffraction spots. However, the {111} cross section which is perpendicular to the line of apsides of the projected ω-phases within a β-phase has not been studied directly. Even with the cross-sectional observation technique (Marcus & Sheng, 1983), which can be carried out by cutting the specimens in the preferred direction with a diamond saw after molding with epoxy resin and then thinning by ion milling, the structure of the cross section could not be investigated. This is due to the fact that, in the cross-sectional direction, the ω-phases concerned do not produce any characteristic diffraction spots, or any contrast in the electron microscope images because the displacement vectors of atoms **b**, which produce the ω-phases, become parallel to the incident beam. However, calculations of the diffracted wave intensity and of the image contrast in the $[10\bar{1}]$ direction as a function of the thickness and the depth of the ω_1- and ω_2-phases can be used to estimate their thicknesses and positions, and also to understand the mechanism of the appearance of the forbidden reflections.

In this paper, the intensities of diffracted waves for specimens with various types of combination of ω-

0108-7681/92/050622-06$06.00